The results of the 2 methods (Equations 5.33 and 5.34) are given below in Table 5.8.

d/D	Pu (kPa)	THEORETICAL NO. OF BUBBLES/kg (EQN. 5.33)	THEORETICAL NO. OF BUBBLES/kg (EQN. 5.34)
0,206	2000	$72,9 \times 10^6$	
	7000	356×10^6	
0,276	2000	126×10^6	
	7000	316×10^6	
0,330	2000	144×10^6	$47,62 \times 10^3$
	7000	174×10^6	
0,377	2000	115×10^6	
	7000	456×10^6	
0,444	2000	226×10^6	
	6000	420×10^6	

TABLE 5.8 BUBBLES PRODUCED AT ORIFICE

From a comparison of the calculations of the theoretical number of bubbles in Table 5.8 above, it can be seen that there is a discrepancy between the two calculation methods used, the energy required method (Equation 5.33) giving bubble production numbers which are in excess of those calculated from the volume method (Equation 5.34). Assuming that the limitations and assumptions used in the foregoing analyses are correct, the results imply that at the incipient cavitation condition, the jet or annulus from the orifice is full of bubbles.

However, the discrepancy between the bubble numbers of the two methods also implies that there is physically insufficient space for all of the bubbles to fit into the orifice flow.

It would hence appear that the assumptions regarding the bubble mass and critical radius require modification. Within the turbulent flow regions immediately upstream and downstream of the orifice, the bubble shape is suspected to be anything but spherical, the turbulence continuously deforming the assumed shape. Therefore, this criterion would also appear to require development. The changing pressures downstream of the orifice would also modify the calculated result. Furthermore, all kinetic energy gained in the process of contraction to the orifice jet (as given in Eqn 5.32) may not be available for bubble formation. This conclusion in some ways agrees with that reported in Section 2.1.3 (Hammitt F.G. 1963), namely that separate energy levels are required for different cavitation levels.

5.3.2 DERIVATION OF INCIPIENT CAVITATION PREDICTION EQUATION

From Section 5.2.3 it was concluded that an incipient cavitation prediction equation should be based on the values of upstream pressure, orifice diameter ratio and pressure drop:

$$\text{Incipient cavitation} = f(Pu, \Delta P, d/D) \qquad 5.35$$

Thus, for one orifice ratio and upstream pressure, incipient cavitation is brought about at a particular pressure drop, therefore

$$\Delta P = f(Pu) \qquad 5.36$$

any given orifice size

$$\Delta P = f(Pu, d/D) \qquad 5.37$$

This result accords with the equation proposed by Ball J.W. et al (1975), viz,

$$V = 0{,}94\, V_R \left(\frac{P_U - P_V}{P_{UR} - P_{VR}}\right)\left(1 - \frac{\log d/D}{10^{[0{,}4 - 0{,}52 \log C_d]}}\right) \qquad 5.38$$

One particular property of the prediction equation is that when the upstream pressure is in fact the vapour pressure, the pressure drop required to cause cavitation is zero.

I.e. if $P_U = P_V$

then $\Delta P = 0$

Hence, the equation must pass through the datum of "zero" pressure ("zero" pressure in this particular case being defined as the vapour pressure of the liquid) and zero pressure drop (alternative representations of ΔP are in terms of velocity and Reynolds Number).

A curve fitting exercise was therefore carried out for the experimental cavitation data calculated from the East Driefontein data, Table 5.4. This exercise showed the best fits (Tables 5.9 and 5.10, and Figures 5.25 and 5.26) to be linear when based on the correlation coefficient, r^2; and logarithmic when based on the root mean square deviation. However, the logarithmic curves are in error when extrapolated below 2000 kPa, in the light of the results of Ball J.W. et al (1975). The linear fits are also inconsistent with the predicted data from Ball J.W. et al (1975) (Figures 4.6 and 4.11) as they have positive intercepts ranging between 159 kPa and 363 kPa, despite their good fit to the incipient cavitation data. Of the remaining two fits, exponential and power curves, the better fit was the power one, which also has the property of passing through the datum zero and is consistent with the predicted data from Ball J.W. et al (1975). For this reason, and contrary to conclusions regarding the fits of the linear and logarithmic curves, the power curve was selected to form the basis of the prediction equation, the resulting curve having the form

$$\Delta P = aP_U^{\ b} \qquad 5.39$$

EQUATION		ORIFICE DIAMETER RATIO, d/D				
		0,206	0,276	0,330	0,377	0,444
LINEAR	r^2	0,98	0,98	0,96	0,93	0,77
	Root Mean Sqaure Deviation	164	162	230	285	366
POWER	r^2	0,98	0,98	0,96	0,93	0,67
	Root Mean Square Deviation	195	187	303	302	429
EXPONENTIAL	r^2	0,98	0,99	1,00	0,89	0,63
	Root Mean Square Deviation	352	370	492	299	307
LOGARITHMIC	r^2	0,92	0,90	0,86	0,88	0,80
	Root Mean Square Deviation	217	93	86	328	465

TABLE 5.9 ERRORS FOR THE DERIVED PREDICTION EQUATIONS

EQUATION	COEFFICIENTS	ORIFICE DIAMETER RATIO, d/D 0,206	0,276	0,330	0,377	0,444
LINEAR	a	0,75	0,63	0,65	0,5	0,43
	b	327,13	363	169	134	374
POWER	a	1,39	1,2	0,42	0,77	10,49
	b	0,94	0,94	1,06	0,96	0,64
EXPON	a	1238,3	1085,5	915,1	779,3	923,14
	b	2,26 x 10-4	2,24 x 10-4	2,5 x 10-4	2,31 x 10-4	1,92 x 10-4
LOGAR	a	-21173,68	-18032,3	-18938,9	-14146,5	-9531,96
	b	2984,95	2549,3	2644,2	1985,7	1412,7

EQUATION TYPES:

Linear $\Delta P = a P_U + b$

Power $\Delta P = a P_U^{b}$

Exponential $\Delta P = a e^{b P_U}$

Logarithmic $\Delta P = a + b \ln P_U$

TABLE 5.10 PREDICTION EQUATION COEFFICENTS

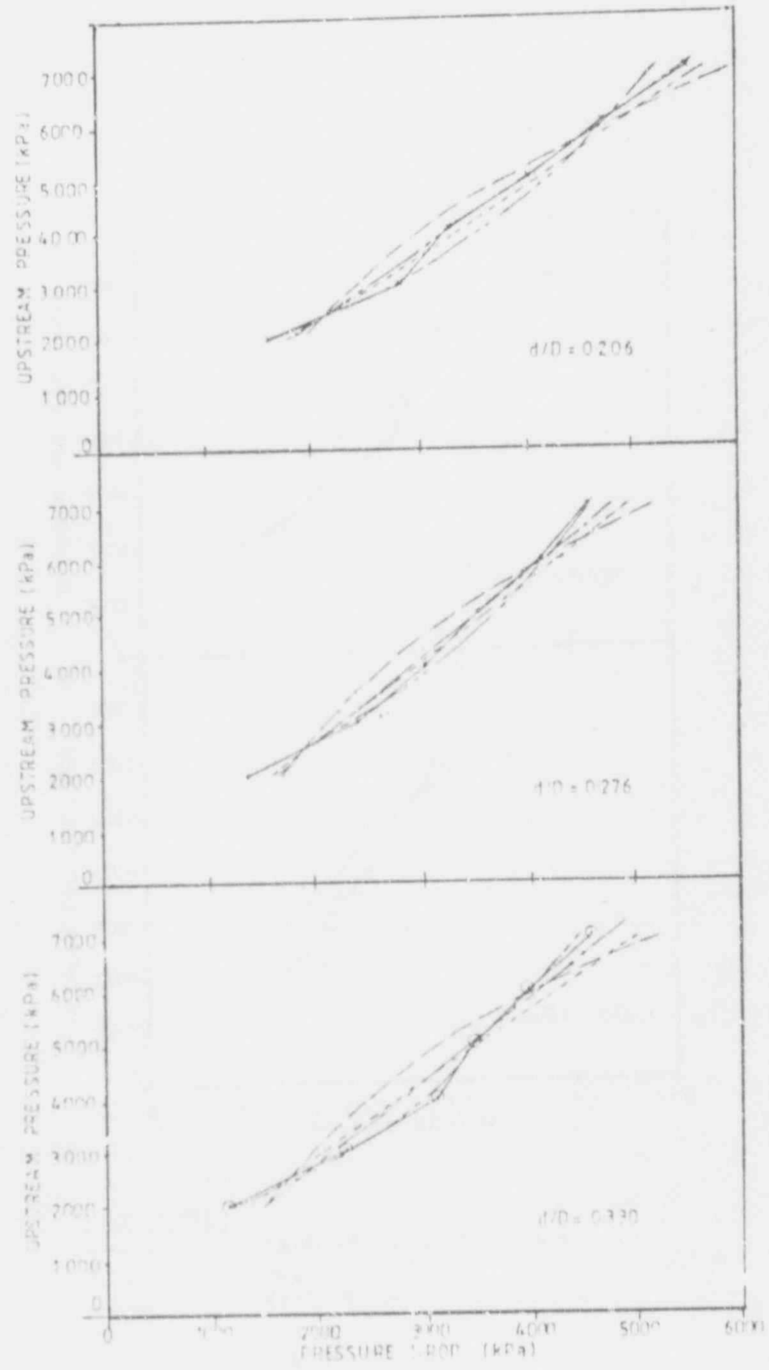

FIGURE 5.25 CURVE FITS FOR INCIPIENT CAVITATION DATA - EAST DRIEFONTEIN GOLD MINE

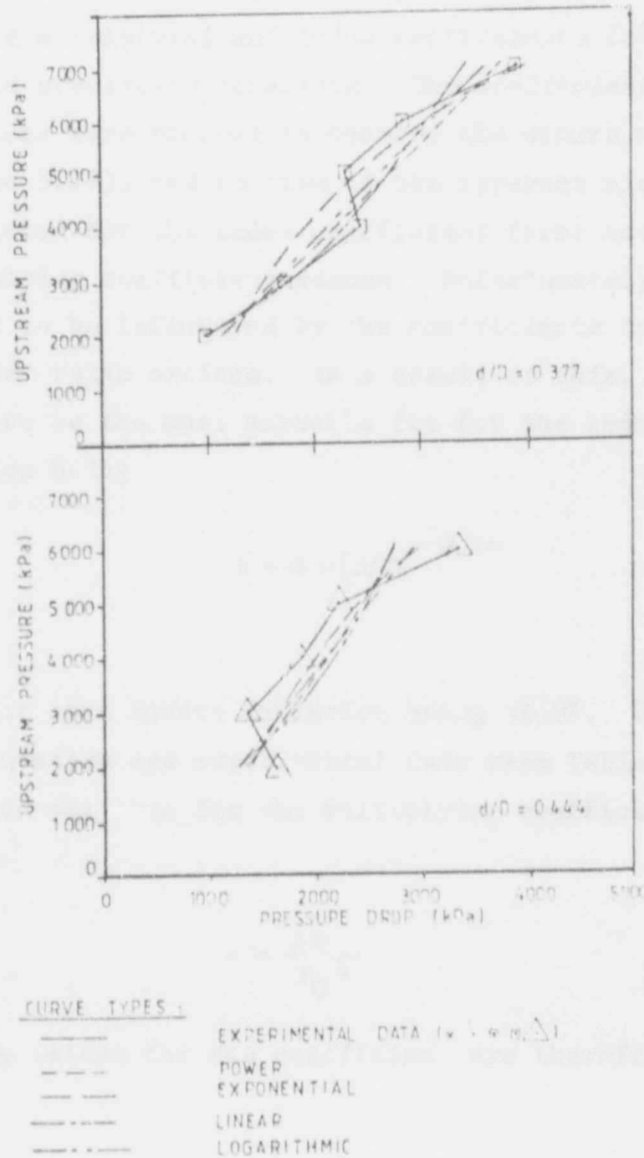

FIGURE 5.26 CURVE FITS FOR INCIPIENT CAVITATION DATA - EAST DRIEFONTEIN GOLD MINE

The coefficients for the various equation fits are shown in Table 5.10.

The next stage of the prediction equation analysis was to generalize the equations for individual orifices into one equation. This was achieved by fitting equations to the derived multiplying and index coefficients for the individual orifice prediction equations. The coefficients for the equations were plotted to observe the nature of their trends (Figure 5.27), and in view of the apparent slopes, an equation was fitted for the index coefficient first and for the multiplying coefficient second. Unfortunately, the graphs appear to be influenced by the coefficients for the 0,444 diameter ratio orifice. As a result of this, [illegible]wer curve was found to be the most suitable fit for the inde[illegible]efficent, the equation being

$$b = 0,6\,(d/D)^{-0,35}$$

the root mean square deviation being 16,9%. Using data from this equation and experimental data from Table 5.4, a new estimate was made for the multiplying coefficient:

ie.

$$a = \frac{\Delta P}{P_U{}^{b}}$$

The new values for the coefficient are therefore

d/D	0,206	0,276	0,330	0,377	0,444
a	0,58	1,16	1,79	1,[illegible]	2,88

and these are shown in Figure 5.28. A linear equation was fitted to this data, the root mean square deviation being 6,6%; the equation is then

$$a = 9,42\ d/D - 1,4$$

The coefficients for the various equation fits are shown in Table 5.10.

The next stage of the prediction equation analysis was to generalize the equations for individual orifices into one equation. This was achieved by fitting equations to the derived multiplying and index coefficients for the individual orifice prediction equations. The coefficients for the equations were plotted to observe the nature of their trends (Figure 5.27), and in view of the apparent slopes, an equation was fitted for the index coefficient first and for the multiplying coefficient second. Unfortunately, the graphs appear to be influenced by the coefficients for the 0,444 diameter ratio orifice. As a result of this, a power curve was nd to be the most suitable fit for the index coefficent, the uation being

$$b = 0{,}6\,(d/D)^{-0{,}35}$$

the root mean square deviation being 16,9%. Using data from this equation and experimental data from Table 5.4, a new estimate was made for the multiplying coefficient:

ie.

$$a = \frac{\Delta P}{P_U^{\,b}}$$

The new values for the coefficient are therefore

d/D	0,206	0,276	0,330	0,377	0,444
a	0,58	1,16	1,79	1,97	2,88

and these are shown in Figure 5.28. A linear equation was fitted to this data, the root mean square deviation being 6,6%; the equation is then

$$a = 9{,}42\, d/D - 1{,}4$$

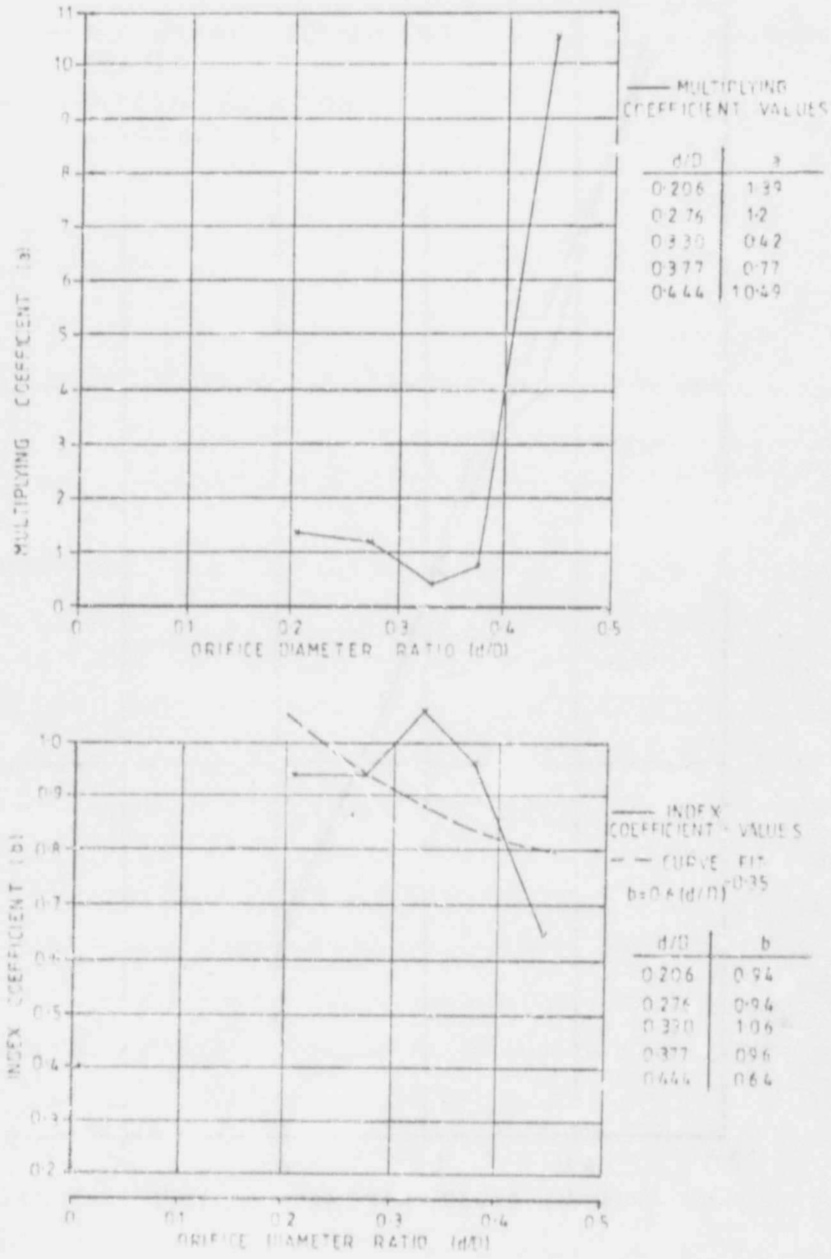

FIGURE 5.27 PREDICTION EQUATION COEFFICIENTS

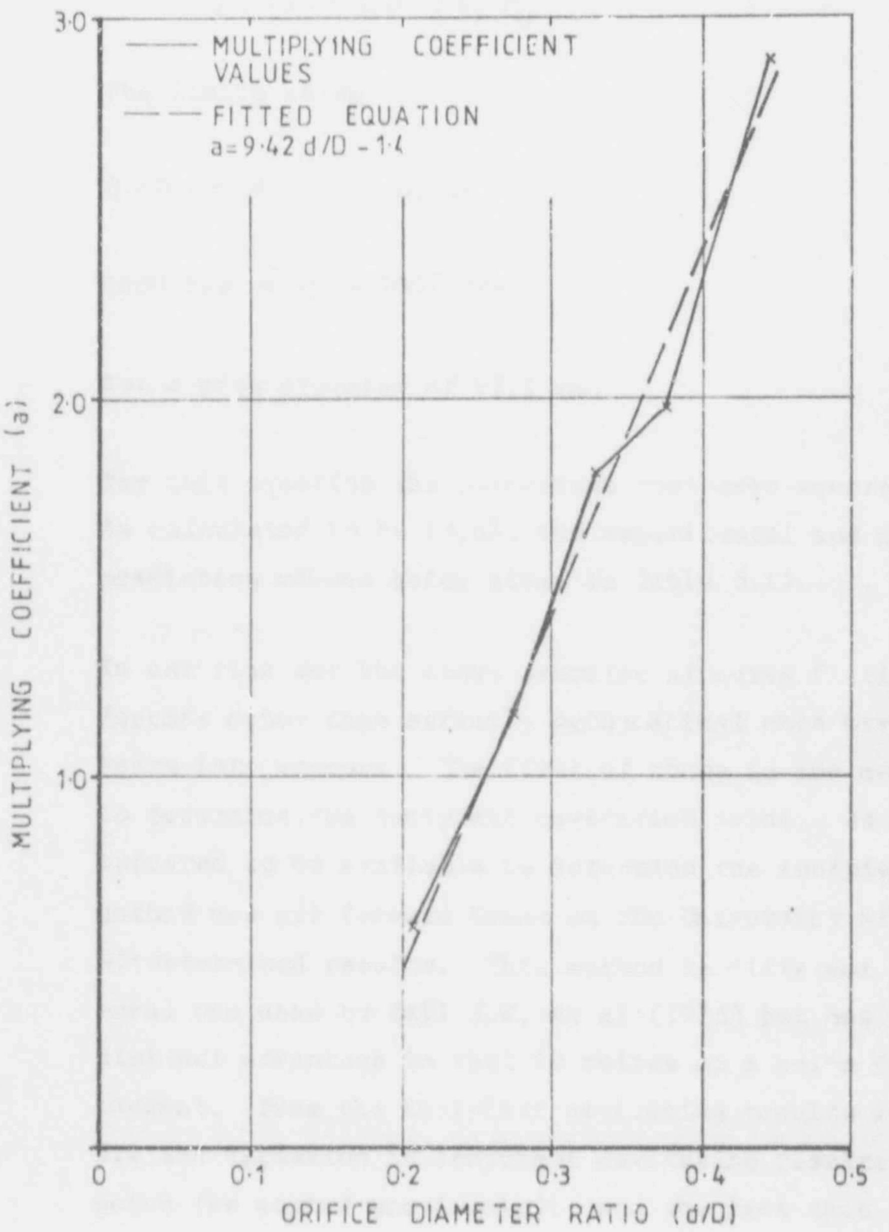

FIGURE 5.28 MULTIPLYING COEFFICIENTS EQUATION

Combining these equations with equation 5.39, the prediction equation becomes

$$\Delta P = (9{,}42\ d/D - 1{,}4)\ F_U^{\ 0{,}6(d/D)^{-0{,}35}}$$

the limits being

0,206 < d/D < 0,444

2000 kPa < Pu < 7000 kPa

for a pipe diameter of 97,2 mm.

For this equation the percentage root mean-square deviation is calculated to be 13,6%, the experimental and calculated prediction values being given in Table 5.11.

In carrying out the above exercise of curve fitting, factors other than strictly mathematical ones have been taken into account. The first of these is the means used to determine the incipient cavitation point. As no method appeared to be available to determine the incipient point a method was put forward based on the University of the Witwatersrand results. This method is different from the aural one used by Ball J.W. et al (1975) but has one distinct advantage in that it relies on a curve fit and a tangent. From the incipient cavitation results in Table 5.4 the variation in incipient cavitation results can be noted (as stated previously); and the fact that the predicted values do not agree completely with the experimental calculated values should be considered in the light of the reasons discussed in Sections 4.1.2 and 5.1.

Further, the methods used to form equations for the index and multiplying coeffients in the prediction equation have tended to smooth the data, thus moving the predicted values away from the experimental ones. This has also focussed attention on another factor, namely, that of equation

d/D		UPSTREAM PRESSURE (kPa)					
		2000	3000	4000	5000	6000	7000
0,206	EXP	1609	2850	3317	4065	4711	5569
	PRED	1497	2286	3086	3894	4710	5531
0,276	EXP	1377	2429	3050	3542	4134	4668
	PRED	1544	2263	2968	3661	4348	5027
0,330	EXP	1147	2226	3109	3491	3975	4555
	PRED	1416	2026	2613	3184	3740	4285
0,377	EXP	1013	1792	2462	2308	2860	3914
	PRED	1314	1849	2359	2847	3320	3782
0,444	EXP	1619	1390	1862	2205	3351	-
	PRED	1187	1643	2066	[illegible]466	2852	-

TABLE 5.11 EXPERIMENTAL AND PREDICTED INCIPIENT CAVITATON VALUES - EAST DRIEFONTEIN GOLD MINE

accuracy. To produce a high accuracy prediction equation which agreed exactly with the experimental results might in itself be misleading, due to the apparent variation in results compared with the trends forecast from upstream pressure and those stated above.

To provide a check on the prediction equation, cavitation limits were therefore predicted for the orifices used in the University of the Witwatersrand experiments. These values are given below in Table 5.12.

	ORIFICE DIAMETER RATIO, d/D			
	0,24	0,43	0,61	0,79
PREDICTED (kPa)	290	295	229	136
EXPERIMENTAL (kPa)	359	214	234	115
Ball J.W. et al (1975) (kPa)	485	182	81	29

TABLE 5.12 EXPERIMENTAL AND PREDICTED INCIPIENT CAVITATION VALUES - UNIVERSITY OF THE WITWATERSRAND

As can be seen, none of the values agree closely, either with the work of Ball J.W. et al (1975) or the derived prediction equation. This again raises doubt as to the definition of incipient cavitation used. Further to this it must also be realised that the test parameters for the University of the Witwatersrand work are outside the limits for the derived prediction equation, whereas those of Ball J.W. et al (1975) are not. Other reasons for the discrepancies are the actual measurements and the physical condition of the pipes and orifices used.

The measurement of flow in both the University of the Witwatersrand and East Driefontein experiments showed reasonably good agreement with theory; however, there was some deviation. This could not be ascribed to a systematic error, as the error was not consistent in all cases for the two experiment sites. Allied to this is the fact that the experimental flowrates forming the basis of the work of Ball J.W. et al (1975) are not known.

Coupled to the above is a certain aspect of pressure drop measurement: this is that the information in Section 5.1.2 shows the pressure drop measurements in the University of the Witwatersrand experiments to become more inaccurate as the pressure drop decreases; and likewise for the East Driefontein experiments - though the latter still remain within acceptable limits. It is also possible that due to the condition of the pipes, the measure pressure drop could have been greater or less than that measured by Ball J.W. et al (1975). The perspex pipes used in the University of the Witwatersrand experiments were smooth and would have a roughness factor that was similar to, or better than, that of steel pipes, this factor possibly changing with pipe age and water residence time (i.e. when no experiments were taking place). With the East Driefontein experiments the pipes installed were new, and had clean and smooth internal surfaces. However, a period of approximately two months elapsed before the test facility was used for the experiments. During this period some water may have entered the pipes and caused rusting. Further, some pipe work modifications had to be carried out after the system was first operated at its design conditions. This meant that the pipes may have been full of water for a further month, and obviously water remained in the pipes between experiments. The effect of the water may have been to erode (rust) the internal surfaces of the pipes and/or cause scale to be deposited on the internal surfaces. Both erosion and scaling would change the roughness characteristic. A higher pressure drop than that calculated could thus be expected (this would also have had the effect of altering the experimental flow/pressure drop curves).

The measurement of flow in both the University of the Witwatersrand and East Driefontein experiments showed reasonably good agreement with theory; however, there was some deviation. This could not be ascribed to a systematic error, as the error was not consistent in all cases for the two experiment sites. Allied to this is the fact that the experimental flowrates forming the basis of the work of Ball J.W. et al (1975) are not known.

Coupled to the above is a certain aspect of pressure drop measurement: this is that the information in Section 5.1.2 shows the pressure drop measurements in the University of the Witwatersrand experiments to become more inaccurate as the pressure drop decreases; and likewise for the East Driefontein experiments - though the latter still remain within acceptable limits. It is also possible that due to the condition of the pipes, the measure pressure drop could have been greater or less than that measured by Ball J.W. et al (1975). The perspex pipes used in the University of the Witwatersrand experiments were smooth and would have a roughness factor that was similar to, or better than, that of steel pipes, this factor possibly changing with pipe age and water residence time (i.e. when no experiments were taking place). With the East Driefontein experiments the pipes installed were new, and had clean and smooth internal surfaces. However, a period of approximately two months elapsed before the test facility was used for the experiments. During this period some water may have entered the pipes and caused rusting. Further, some pipe work modifications had to be carried out after the system was first operated at its design conditions. This meant that the pipes may have been full of water for a further month, and obviously water remained in the pipes between experiments. The effect of the water may have been to erode (rust) the internal surfaces of the pipes and/or cause scale to be deposited on the internal surfaces. Both erosion and scaling would change the roughness characteristic. A higher pressure drop than that calculated could thus be expected (this would also have had the effect of altering the experimental flow/pressure drop curves).

The last reason is that of the orifice profile, the orifice for the University of the Witwatersrand tests being machined from brass and those for East Driefontein from alloy steel (EN 58) which was then heat treated to ensure minimal damage due to cavitation erosion because of possible test duration. It was evident from examination of the orifices before and after use that the leading edge profile had not changed. All of the orifices had a slight rounding of the leading edge after manufacture, the radius being typically of the order of 0,3 mm. Using Miller D.S. (1971), an estimation of the effect of this edge radius on orifice performance was made. For the 8,2 mm diameter orifice the true pressure drop would be a factor of 1,1 times that measured, and for the 43,2 mm orifice the pressure drop would be 1,04 times that measured.

From the above discussions and the Sections on results for the University of the Witwatersrand and East Driefontein experiments, and in particular, on the differences between experimental, predicted (Ball J.W. et al, 1975) and derived prediction equation results, it is clear that calculated errors have not generally been of sufficient magnitude to account for the differences. In such instances further reasons have been put foward to account for the differences. Outside of these there remains a further factor, that of temperature. The experimental facilities were operated at different temperatures, and the temperatures applicable to the work of Ball J.W. et al (1975) are not known. Although undetermined, this aspect may have affected results. Taking the East Driefontein results for instance, with a water temperature of 24°C, then if the temperature had been above this, the water vapour pressure would have been higher and one would expect cavitation to occur more easily. However, if the temperature had been lower, it would have been expected that cavitation would be harder to achieve.

In view of the differences between the original definition of incipient cavitation and the one proposed and used herein, discrepancies of one kind or another are bound to occur. However, it is felt that the method used to determine incipient cavitation is still of value, and by utilising the incipient cavitation point instead of that corresponding to critical, incipient damage, or choking, conditions, a certain margin of safety has been built into the results of the experiments. The defined incipient point acts as a 'go no-go gauge', any flow or pressure drop up to the incipient point indicating operation with no cavitation, and above it indicating cavitation.

In the following section the derived prediction equation for incipient cavitation is applied to establish various design criteria.

6. APPLICATION OF ANALYSIS TO DESIGN

The problem as discussed in Chapter 1 was primarily one of determining a method for predicting cavitation limits for an orifice (the orifice being the means proposed to effect pressure dissipation) - in other words, to serve as a design guide. The derived prediction equation is:

$$\Delta P = (9{,}42\, d/D - 1{,}4)\, P_U^{\,0{,}6(d/D)^{-0{,}35}} \qquad 6.1$$

Any prediction method used should be relatively easy to apply and be capable of providing data on pressure losses in the limiting case, i.e. when cavitation actually occurs. After an examination of possible forms of data presentation - nomograph, graph, equation, data table, etc. - it was decided that the most suitable form would be the graphical one, the reason being that a graph can be conveniently used to present a large amount of readily assimilable information on a single sheet. The information thus presented would enable the process of pressure dissipation and cavitation limits to be viewed together. The level of interpolation required can also easily be judged from the shape of the curves shown on the graph, and any extra data that may be required can be superimposed later.

To comply with the above format the graph in Figure 6.1 was constructed. Essentially it is the pressure drop/flowrate graph for the orifices tested at East Driefontein Gold Mine. Superimposed on the graph are curves which have been drawn using the derived incipient cavitation prediction equation (Section 5.3.2), each curve representing the incipient cavitation limit for the upstream pressure condition of each orifice used. For any particular point on a cavitation curve there is thus a cavitation area and a non-cavitation area. The cavitation area is the part of the pressure drop/flowrate curve for the particular orifice in question that is above the cavitation curve, and any pressure drop/flowrate given by this line will result in a cavitating condition. The non-cavitation area is

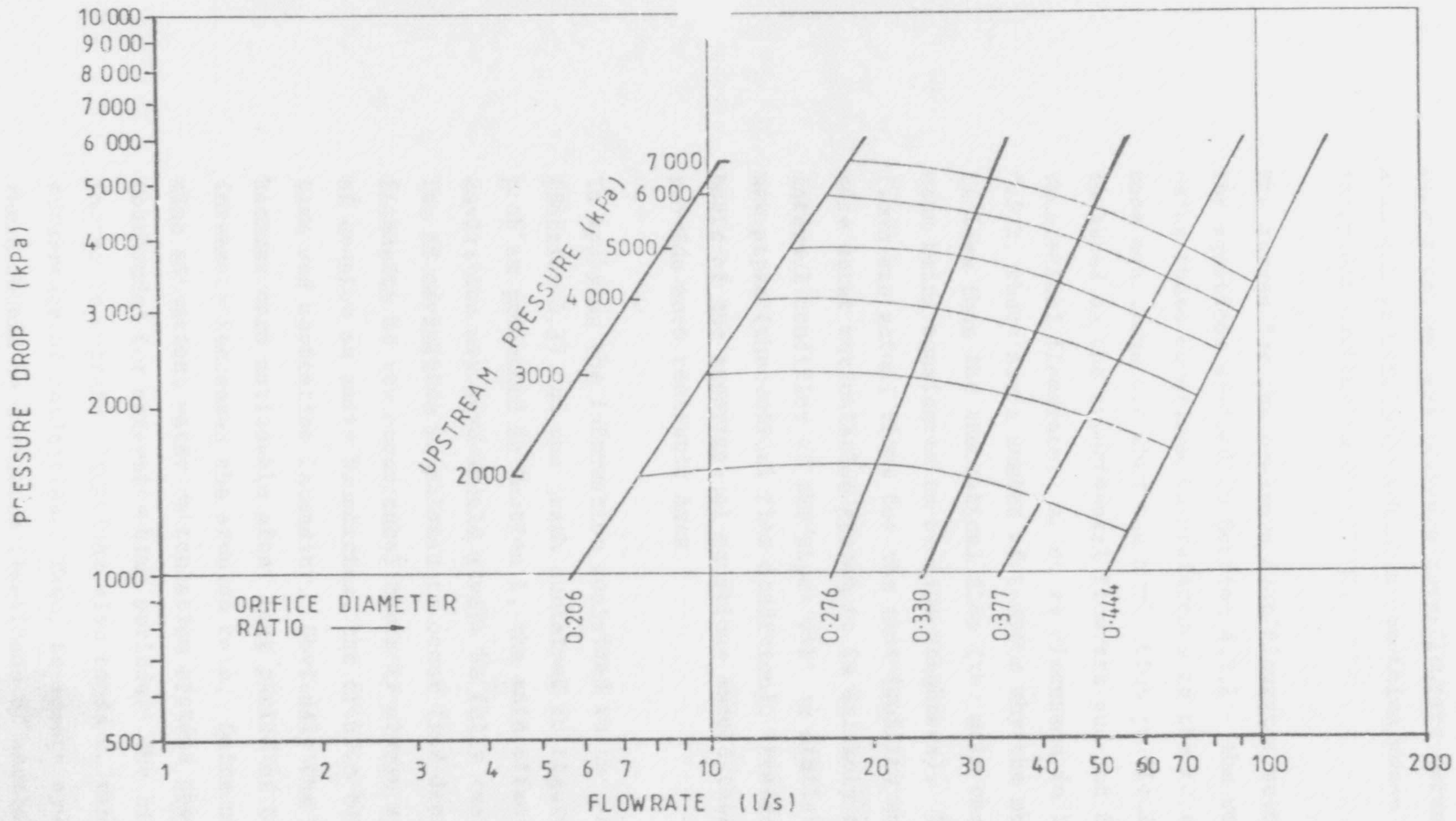

FIGURE 6.1 PREDICTION GRAPH FOR ORIFICE INCIPIENT CAVITATION

below the cavitation curve and also follows the pressure drop/flowrate curve for the particular orifice. This is a safe area, and any pressure drop/flowrate curve within this area can be utilised without a condition worse than incipient cavitation occurring.

The curves for the pressure drop/flowrates were drawn using the equations derived in Section 4.2.2; the reasons for using these equations in preference to the accepted text book equations are that the cavitation prediction equation is based on the experimental flowrate and not the theoretical flowarate. Also, as discussed in Section 5.3.3, there are a number of reasons why the measured flow is less than the theoretical flow (the main one in this case being considered to be pipe roughness). Thus measured flows are actual flows for the test facility and in any mine water reticulation system it is unlikely that the internal condition of the pipes will be similar to that of new pipes (theoretical flow condition). Prediction on the basis of the experimental equations should therefore provide more realistic data.

In applying the information contained in the analysis (Section 5.3) and the graph contained in Figure 6.1 to the problem presented in Section 1, the main effect which cavitation may have should always be fully realised. This is, if cavitation is allowed to occur (and depending on the intensity of its occurrence) there is always a possibility of erosion on solid boundaries, the erosion being linked to time and cavitation intensity. Obviously the erosion becomes more noticeable after long period of time, while intensity increases the erosion rate. Quite often in the mine situation, water reticulation systems operate unattended for extensive time periods. The high noise factor in certain situations also tends to mask the occurrence of cavitation. Thus, to ensure system integrity there should be a minimum likelihood of cavitation occurring, or the cavitation level should be such that no damage will occur, i.e. incipient cavitation is the worst case allowable.

6.1 APPLICATION OF DESIGN DATA TO MINING PROBLEMS

To demonstrate the use of the design data in Section 6, two examples are given below. These are not the only cases where cavitation could occur in a water reticulation system; however, it is felt that they ably demonstrate the use and application of the experimental data conveyed in Figure 6.1.

Example (i)

Water at a flowrate of 50 l/s is required to fill a dam downstream of a Pelton turbine. The water is drawn from the shaft column and the turbine is at a depth of 714 m below the surface (the static pressure available being 7000 kPa). The decision having been taken to use an orifice plate pressure dissipator to act as the turbine bypass, it is thus required to size the orifice plates needed for the pressure dissipator, given that the back pressure produced by the pipework downstream of the orifice is 700 kPa at 50 l/s. No cavitation - other than incipient cavitation - should be allowed to occur.

Solution

From Figure 6.1 it will be noted that higher pressure drop/upstream pressure ratios can be achieved with the smaller orifice sizes. The flow through the orifice will then be as small as possible. Making the assumption that a group of 2 orifices in parallel will be suitable for pressure dissipation, the flowrate per orifice will be 25 l/s, at which value the maximum pressure drop for an upstream pressure of 7000 kPa is 5380 kPa, the orifice diameter ratio then being 0,239. Therefore, after the water has passed through the first set of orifices the pressu[illegible]comes 1620 kPa, and the pressure which is still re[illegible] dissipated is 920 kPa. The maximum pressure [illegible] dissipated at 25 l/s and 1620 kPa is 1300 kPa, the [illegible] diameter ratio then being 0,271. Thus, the

920 kPa can be dissipated by an orifice operating below the incipient cavitation point, i.e. one of 0,34 orifice diameter ratio (it is evident that the 2 flows rejoin after this point and flow to the dam as one). The pressure is thus reduced to 700 kPa, which is suitable for the downstream pipe work. This process is summarised below in Table 6.1 and Figure 6.2.

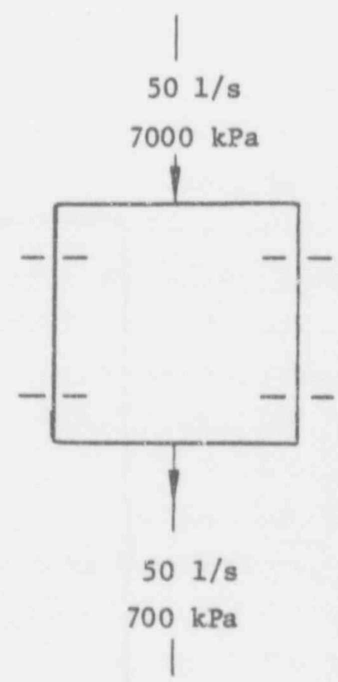

UPSTREAM PRESSURE (kPa)	PRESSURE DROP (kPa)	d/D	ORIFICES REQUIRED	FLOW (l/s)
7000				
	5380	0,239	2	25
1620				
	920	0,34	2	25
700				

TABLE 6.1 SUMMARY OF SOLUTION TO EXAMPLE (i)

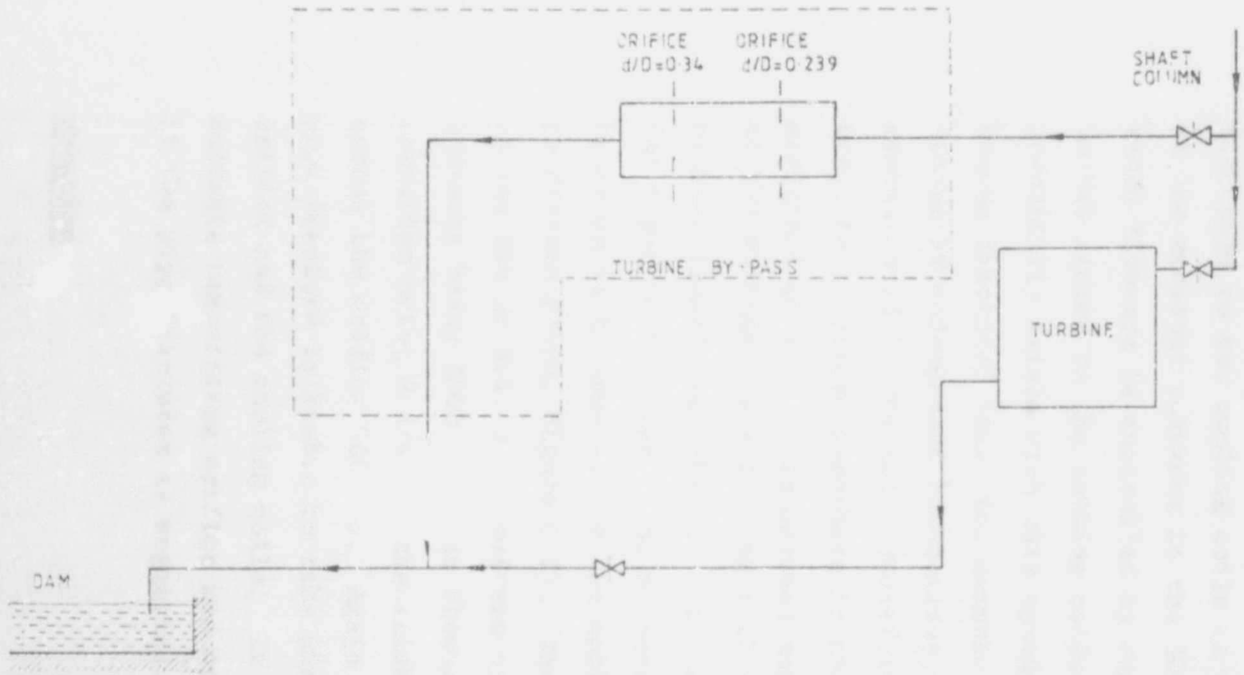

FIGURE 6.2 SCHEMATIC DIAGRAM OF TURBINE BY-PASS FOR EXAMPLE (i)

Example (ii)

Water is fed via the shaft column (and a pressure reducing valve) to a particular level of a mine. At that level, the water flows through a 150 mm N.B. pipe until the first crosscut, whence some of the water flows through a 100 mm N.B. pipe to two cooling coils (a main valve being situated at the crosscut entrance in the 100 mm N.B. pipe). The water flowrate is controlled by constant flow control valves fitted to the cooling coils (Figure 6.3). The possibility exists with this system that if a pipe should become fractured (due, for example, to a fall of rock, damage by underground locomotives, etc.), the entire water system could be drained. Therefore, a restricting orifice needs to be placed somewhere in the reticulation system described above. It is assumed that the pipe will fracture at the entrance to a cooling coil - the valves being located downstream (this is not the only possible location for pipes to fracture; the purpose of this choice of location is to demonstrate the application of the prediction graph, Figure 6.1). The orifice is to be placed in the 100 mm N.B. pipe upstream of the cooling coils, the pressure being 2000 kPa, the flowrate during normal operation being 8 l/s and the allowable pressure drop across the orifice 500 kPa. Again it is assumed that a pipe fracture is liable to take place somewhere between the orifice and the cooling coils. It is required to size a suitable restricting orifice and to determine the flowrate if the pipe fractures as suggested.

Solution

For an orifice to provide maximum system protection it must be sized for 8 l/s at 2000 kPa for a pressure drop of 500 kPa. Referring to Figure 6.1 this requirement indicates an orifice diameter ratio of 0,243 (8 l/s at 500 kPa). The pressure drop for incipient cavitation at an upstream pressure of 2000 kPa is 1560 kPa; therefore, during normal system operation no cavitation should occur.